

## SOME REMARKS ABOUT STICK-SLIP OSCILLATORS

**Roberta Lima<sup>a,b</sup> and Rubens Sampaio<sup>a</sup>**

<sup>a</sup>*PUC-Rio, Avenida Marquês de São Vicente, 255, Gávea, Brasil*

<sup>b</sup>*Paris-Est, Laboratoire de Modelisation et Simulation Multi Echelle, Equipe de Mecanique, 5, Boulevard Descartes, 77454, Marne-la-Vallee, Cedex 2, France*

*roberta\_10\_lima@hotmail.com, rsampaio@puc-rio.br*

**Keywords:** Friction-induced vibration, stick-slip, non-smooth system, nonlinear-dynamics, stochastic modeling.

**Abstract.** The objective of this paper is to analyze the behavior of a stick-slip dry-friction oscillator in the steady-state solution. The system is composed by a block of mass  $m$  connected to a fixed support by a spring of stiffness  $k$ . The block moves over a continuous belt that is driven by rollers. The frictional force between the block and the belt is modeled as a Coulomb friction. By numerical simulations, different imposed belt velocity and dry-friction configurations are analyzed, from a deterministic and from a stochastic viewpoint. The focus of the paper is finding the stick- and slip-mode parts of the trajectory in the steady-state through the phase diagram. In the stochastic analysis, some parameters of the dry-friction model are considered uncertain. The friction coefficient and the belt speed are modeled as random process and random field respectively. Monte Carlo simulations are employed to compute the statistics of the response of the stochastic differential equation of motion of the stick-slip dry-friction oscillator.

## 1 INTRODUCTION

The motivation for exploring the different aspects of friction must have had its origin in solving practical problems. Friction is not a new subject. It had been a topic of technological attention long before the dawn of science, and is still an important topic in science and engineering today. Study of oscillatory conditions in dry friction systems has practical significance for providing protection against vibrations, seismic isolation, reduction of noise and friction-induced vibration, etc (Feeny et al., 1998; Berger, 2002).

The nature of dynamic friction forces developed between bodies in contact is extremely complex and affected by many factors: the constitution of the interface, inertia and thermal effects, roughness of the contacting surfaces, history of loadings, the presence of lubricants, and many others. Thus, friction is not a simple phenomenon but a collection of many complex mechanical and chemical phenomena (Tariku, 1998; Poudou, 2007).

The friction literature is replete with examples of velocity-dependent friction models, and many of them are a single-coefficient friction model. As a result, predictions of friction using a simplified friction model are far from true.

Beside this, the stick-slip vibrations are self-sustained oscillations induced by dry friction and since the friction can be characterized in two qualitatively different parts (kinetic and static frictions) with a non-smooth transition, the resulting motion also has a non-smooth behavior. Thus, stick-slip systems belong to the class of non-smooth systems, such as systems with stops, impacts and hysteresis (Zaspa, 2009; Csernák and Stépán, 2006).

The friction non-smooth behavior associated with the absence of a universally accepted friction model and the friction coefficient variability (due to the many factors that can affect it), make the stochastic approach the ideal way to deal with friction models. Also, random exists on the real friction system and the friction coefficient possesses random behavior (Feng, 2003).

The main motivation of this paper is to better understand the stick-slip behavior on drilling, that is very complicated and appears during 50% of drilling time (Navarro-López and Suárez, 2004). One of the consequences of the stick mode is that, since a constant speed is imposed at the top of the drillstring and during the stick the bit at the bottom does not move, the drillstring is twisted and acts as a spring. In this paper a simpler model of this process is studied. The model is the bare minimum to study stick-slip. It has a block, modeled as a particle, with mass but no dimension; a spring to give an elastic force; and a belt to drive the system. Between the block and the belt there is dry friction. Of course the results are dependent of the dry friction model used. The dynamics of this simple system can be divided in two parts, a slip and a stick mode. We call stick when the relative velocity of the block-belt is null in a time-interval, not just an instant. If the relative velocity is non-zero, or zero in isolated points, we call slip. The equation of motion has different roles during stick and slip. Indeed, in the stick-mode, the block moves with the same velocity as the belt and the friction force stays within its bounds; the friction force is not known but the acceleration of the block is known as well as its position. The dynamical equation acts as a constraint to find the friction force. In the slip part of the motion one has a standard dynamical problem, solved by integration of the dynamical equation. In the phase plane, while the slip region has non-zero measure, the stick region has zero measure and is a manifold of lower dimension, one or zero.

Stick-slip dynamics appears also in several other situations, as for example in the peeling of an adhesive tape from a roller (Cortet et al., 2013), but due to different reasons. We are only interested in stick-slip caused by dry-friction.

In this paper several different imposed belt velocity and dry-friction configurations are an-

alyzed, from a deterministic and also from an stochastic viewpoint. In the simpler model the belt has constant velocity, but if the belt velocity is not constant the manifold of possibilities for the stick-slip distribution is very rich as, one presumes, in the drilling process. Also, if the coefficient of friction is not constant in the belt, as when it is formed from different materials or same material but with different state of lubrication, even considering Coulomb friction, the dynamics is very rich.

Also, since it is well known that the friction properties of contacting surfaces vary a lot with ambient conditions, as temperature, humidity, state or lubrication, etc, so stochastic modeling is also done. The belt velocity and the friction coefficient are taken as stochastic.

This paper is organized as follows. Section 2 describes a most simple stick-slip oscillator. Section 3 presents the results of the deterministic simulations. The probability models to the uncertain friction force are construct in Section 4 and the results of the simulations of the stochastic system are presented in Section 5. Section 6 presents some conclusions.

## 2 DETERMINISTIC MODEL OF THE STICK-SLIP OSCILLATOR

The system analyzed in this paper is composed by a block connected to a fixed support by a spring. The block moves over a continuous belt that is driven by rollers, as shown in Fig. 1.

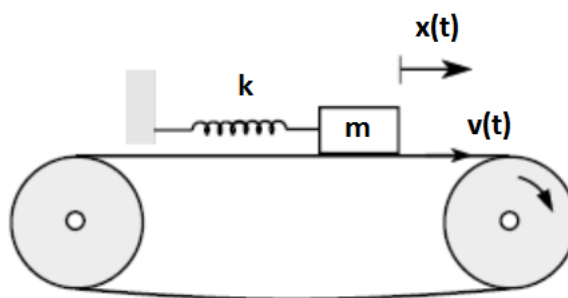


Figure 1: Stick-slip oscillator

The position of the block over the belt is represented by  $x$  and its equation of motion is

$$m\ddot{x}(t) + kx(t) = f(t), \quad (1)$$

where  $m$  is the mass of the block,  $k$  is the spring stiffness and  $f$  is the frictional force between the block and the belt. The belt speed is represented by  $v$  and it is assumed that  $f$  depends on the slip velocity,  $v - \dot{x}$ , as

$$f(t) = n\mu \operatorname{sgn}(v(t) - \dot{x}(t)), \quad (2)$$

where  $n$  is the normal force exercised by the belt on the block and  $\mu$  is the friction coefficient. In a simple friction model, this coefficient can be assumed constant, but more sophisticated models assume that  $\mu$  is a function of the slip velocity, for example, a cubic function (Vahid-Araghi and Golnaraghi, 2010)

$$\mu(v) = \mu_0 - \mu_1 |v| + \mu_3 |v|^3, \quad (3)$$

with  $\mu_0, \mu_1, \mu_3 > 0$ . Next is presented the analysis of the solution of a simple problem, in it the belt velocity is imposed and has a constant speed. To better understand what is stick-slip,

the analytical results of the simple stick-slip oscillator with a belt with a constant speed will be later compared to the numerical results of the stick-slip oscillator in the case of imposed non-constant velocity.

Considering that the belt speed and  $\mu$  are constant in time, represented by  $v$  and  $\mu$ , and introducing a new variable  $y = \dot{x}$ , it is possible to write two solutions for the phase paths of the system

$$\begin{aligned} \text{when } y > v \quad y^2 + \omega_n^2 \left( x + \frac{n\mu}{m\omega_n^2} \right)^2 &= c \\ \text{when } y < v \quad y^2 + \omega_n^2 \left( x - \frac{n\mu}{m\omega_n^2} \right)^2 &= c, \end{aligned} \quad (4)$$

where  $c$  is a constant and  $\omega_n$  is the natural frequency of the system. Writing  $z = x\omega_n$ , the phase paths become

$$\begin{aligned} \text{when } y > v \quad y^2 + \left( z + \frac{n\mu}{m\omega_n} \right)^2 &= c \\ \text{when } y < v \quad y^2 + \left( z - \frac{n\mu}{m\omega_n} \right)^2 &= c. \end{aligned} \quad (5)$$

Thus, given a positive  $v$ , the phase diagram of the system, has a single equilibrium point at  $(n\mu/m\omega_n, 0)$ . Given a negative  $v$ , its single equilibrium point is at  $(-n\mu/m\omega_n, 0)$ , as shown in Fig. 2(a) and 2(b). In both cases, it is a centre (Jordan and Smith, 2007).

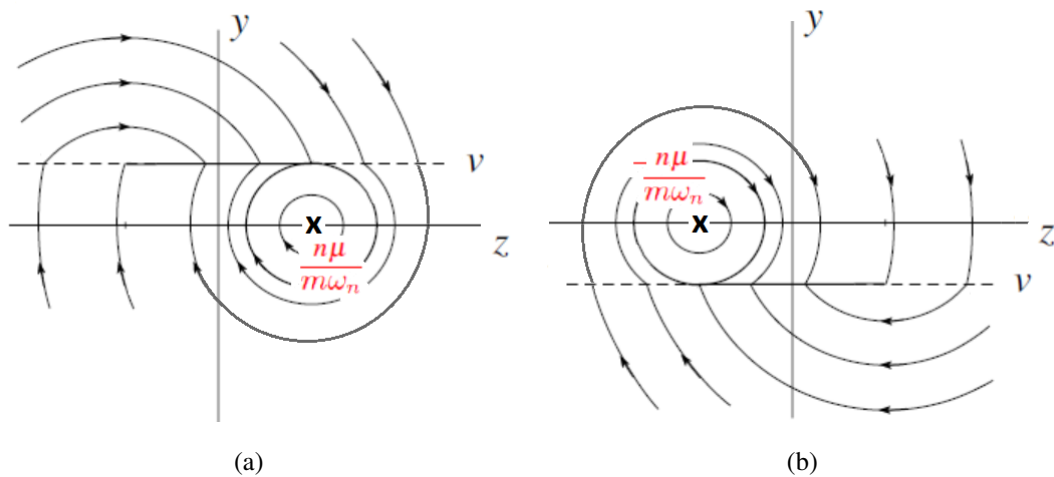


Figure 2: Phase diagram for the stick-slip oscillator with (a) positive and (b) negative belt speed.

The horizontal segment  $y = v$  and  $|x| \leq \mu n/k$  correspond to the stick phenomena, i.e., when the block moves with the belt velocity and the friction force is able to compensate the elastic force to maintain the block put. This phenomena can happens only before the system reach the steady state, because after it, the phase paths are written as a circle with origin in the equilibrium point, Eq. 5, and with radius related with the block initial conditions of the movement. When  $|\dot{x}(0)| \geq |v|$ , the circle radius is  $|v|$ . When  $|\dot{x}(0)| < |v|$ , it is  $\sqrt{\dot{x}(0)^2 + \left( x(0)\omega_n + \frac{n\mu}{m\omega_n} \right)^2}$  if  $\dot{x}(0) > v$ , and it is  $\sqrt{\dot{x}(0)^2 + \left( x(0)\omega_n - \frac{n\mu}{m\omega_n} \right)^2}$  if  $\dot{x}(0) < v$ .

Thus, if we draw the phase diagram of a stick-slip oscillator with a constant belt speed and Coulomb friction, considering only the steady state solution of the system, there is no stick mode. The path will be written as a circle and it has only slip mode. In the case the circle radius is equal to  $|v|$ , the block and the belt will have in the steady state solution the same velocity in an instant, but this is not what it is considered as stick mode.

With different friction models, it is possible have the stick mode during the steady state solution (Galvanetto and Bishop, 1999).

To make a energy analysis in the system in the case in which the belt has a constant speed, we multiply Eq. 1 by  $y$  and integrate it in the interval  $[0, t^*]$  as

$$\frac{my^2(t)}{2} \Big|_0^{t^*} + \frac{kx^2(t)}{2} \Big|_0^{t^*} = \int_0^{t^*} f(t)y(t) dt. \quad (6)$$

Thus, we obtain

$$\frac{my^2(t^*)}{2} + \frac{kx^2(t^*)}{2} = \frac{my^2(0)}{2} + \frac{kx^2(0)}{2} + \int_0^{t^*} f(t)y(t) dt. \quad (7)$$

After, we rewrite Eq. 7 as

$$E_k(t^*) + E_p(t^*) = E_k(0) + E_p(0) + \int_0^{t^*} f(t)y(t) dt, \quad (8)$$

where  $E_k$  and  $E_p$  indicate respectively the kinetic energy and the elastic energy in the system. Thus, calling  $E_m$  the total mechanic energy in the system, we obtain

$$E_m(t^*) = E_m(0) + \int_0^{t^*} f(t)y(t) dt. \quad (9)$$

During the stick-mode, as the block velocity is equal to the belt velocity, the frictional force varies according to the following equation

$$f(t) = k x(t), \quad (10)$$

and it is confined to the interval  $-f_{max} < f < f_{max}$ , where  $f_{max}$  is the maximum static friction force given by the product of the friction coefficient with the normal force, that is,  $f_{max} = \mu n$ .

During the slip-mode, the value of the frictional force,  $f$ , is known and constant. Its absolute value is equal to the maximum friction force,  $\mu n$ . Thus, by Eq. 9 we obtain

$$\begin{aligned} \text{when } y > v \quad E_m(t^*) &= E_m(0) - \mu n(x(t^*) - x(0)) \\ \text{when } y < v \quad E_m(t^*) &= E_m(0) + \mu n(x(t^*) - x(0)). \end{aligned} \quad (11)$$

Observing Eq. 11, we conclude that the frictional force can introduce or dissipate energy in the system. It dissipates energy if the block moves in the opposite direction the belt or moves in the same direction but faster. It introduces energy if the block moves in the same direction but slower.

### 3 NUMERICAL SIMULATIONS OF THE DETERMINISTIC STICK-SLIP OSCILLATOR

To better comprehend the behavior of the stick-slip oscillator when the belt do not have a constant speed and when the friction coefficient changes along the belt length, we started

analyzing some deterministic models. In the first part of the section, simulations with different models of non-constant belt speed are compared with the analytical results (developed for the case in which the belt has a constant speed) in order to observe their influence in the system response, as in the stick and slip mode. In the second part of the section, simulations with variable friction coefficient along the belt length are compared with the analytical results.

In all deterministic and stochastic simulations, Eq. (1) was integrated in a range of [0.0, 200.0] seconds. For the integration, it was used the function *ode45* (based on the Runge-Kutta 4th/5th-order method with a varying time-step algorithm) of the *Matlab* software with a maximal step size equal to  $10^{-4}$  seconds. Also, the maximal absolute error allowed in the integrations was  $10^{-4}$ . Many numerical experiments were done in order to determine this parameter optimal value. The choice of an appropriate value of the error is crucial. When we have a big maximal absolute error, the simulations have a lower computational cost. This is specially important in the stochastic simulations, in which Monte Carlo simulations are employed to compute the statistics, and many similar problems should be resolved. On the other hand, if the maximal absolute error is too big, we compromise the accuracy of the results. As the stick-slip system has a non-smooth behavior, the detection of transitions from one mode of motion to another mode should be done carefully.

The values of the parameters used were 1.0 [Kg] for the block mass, 4.0 [Kg] for the spring stiffness, 1.0 [N] for the normal force, 1.0 for the constant friction coefficient and  $v_0 = 1.0$  [m/s] for the modulus of the belt speed. As initial conditions to the system, it was considered  $x(0) = 0.0$  [m] and  $\dot{x}(0) = 1.0$  [m/s]. These values were used in almost all simulations, when this is not the case specific comments about the parameters are made.

### 3.1 Belt with harmonic speed

The first non-constant belt motion analyzed is when the belt speed is harmonic (Csernák and Stépán, 2006), that is

$$v(t) = v_0 \cos(\omega_b t), \quad (12)$$

where  $v_0$  is the amplitude and  $\omega_b$  is the frequency of the belt speed. In this case, the graph of the phase path in the steady state are not circles. Depending on the ratio  $r = \omega_b / \omega_n$ , it can have more than one equilibrium point and can have the stick mode. To show this different behavior, numerical simulations were done for different values of  $r$ .

As result, it is possible to observe that for small values of  $r$ , the phase diagram of the system response in the steady state has two equilibrium points, as it is shown in Fig. 3(a) and 3(b), where the two equilibrium points are marked with a cross. Around each equilibrium point, the block path is a circle. In 3(b) the two circles are tangent.

As  $r$  increases, approaching 1.0, these two circles overlap, starting to merge, until they coincide for  $r = 1$ , forming a single path with origin at (0,0), as shown in Fig. 4(a) and 4(b). After the ratio  $r$  exceeds de value 1, the position of the equilibrium point do not change anymore, it remains at the origin of the phase diagram, but the circle deforms into a sort of ellipses, Fig. 5(a) and 5(b).

It is important to observe that in all graphs of Fig. 3(a), 3(b), 4(a), 4(b), 5(a) and 5(b), show only the phase path of the system response in the steady state. Also in these graphs, the positions in which  $y = v$  considered as stick mode are marked in red. By them, it is possible to verify that, differently from the case in which the belt has a constant speed, the stick mode can occur in the steady state of the system and do not form anymore, of course, a horizontal straight segment in

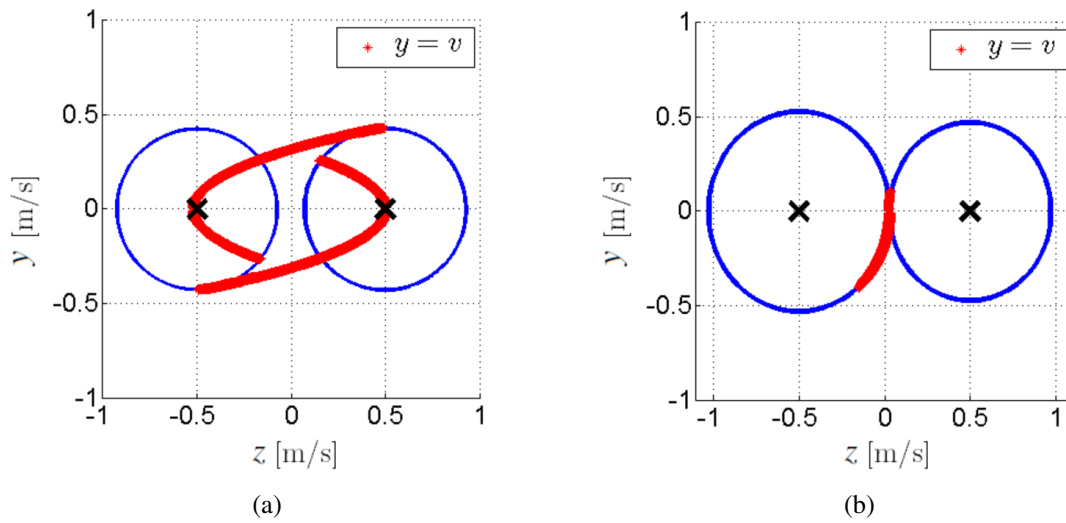


Figure 3: Belt with harmonic speed: phase diagram for the stick-slip oscillator in the steady state with (a)  $\omega_b/\omega_n = 0.1$  and (b)  $\omega_b/\omega_n = 0.5$ .

the phase diagram. For the case  $r = 1.0$ , the stick mode occurs during the entire path, i.e., there is no slip.

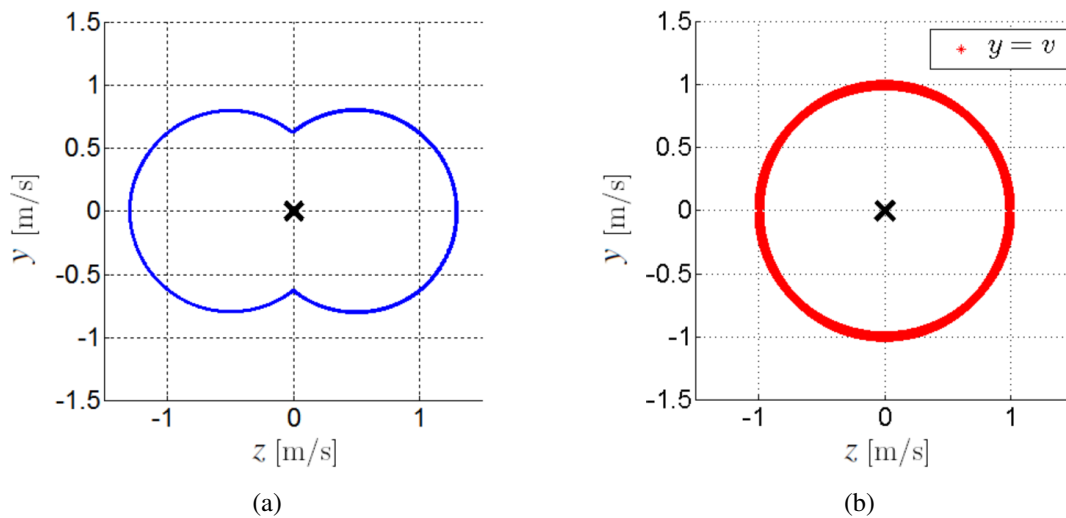


Figure 4: Belt with harmonic speed: phase diagram for the stick-slip oscillator in the steady state with (a)  $\omega_b/\omega_n = 0.7$  and (b)  $\omega_b/\omega_n = 1.0$ .

### 3.2 Belt with non-smooth speed

Now the belt has a periodic (with frequency  $\omega_b$ ) but no non-smooth speed, as follows

$$v(t) = \begin{cases} -v_0, & \text{if } t \in [0, a); \\ \frac{2v_0}{b}t + \frac{v_0(-2a-b)}{b}, & \text{if } t \in [a, a+b); \\ v_0, & \text{if } t \in [a+b, 1/\omega_b). \end{cases} \quad (13)$$

A sketch of this imposed belt speed is shown in Fig. 6. Two different situations of this periodic function are analyzed. In the first one, it is assumed that  $a \rightarrow 0$ , that is, the belt speed

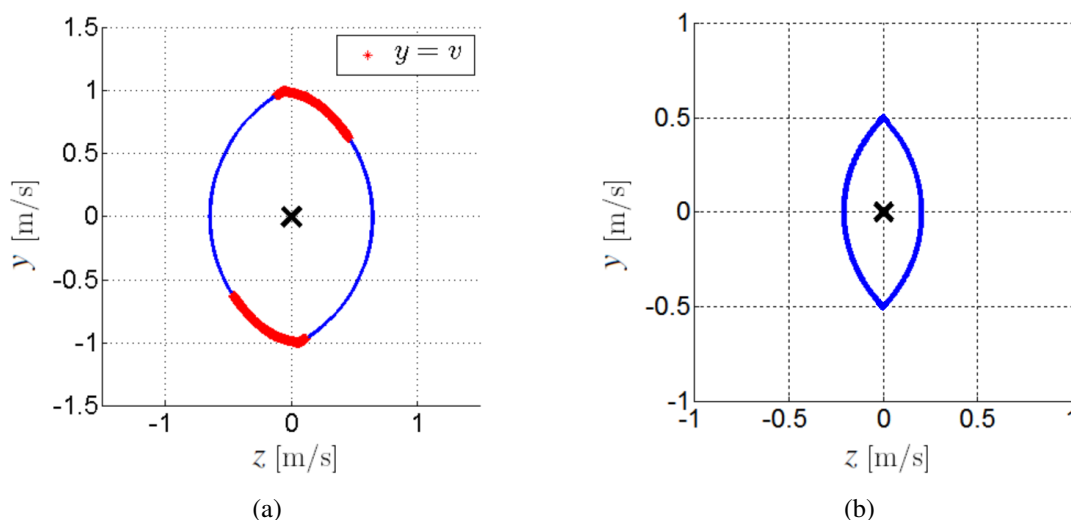


Figure 5: Belt with harmonic speed: phase diagram for the stick-slip oscillator in the steady state with (a)  $\omega_b/\omega_n = 1.4$  and (b)  $\omega_b/\omega_n = 2.0$ .

is a continuous but non-smooth function. In the second one, it is assumed that  $b \rightarrow 0$ , that is, the belt speed is a discontinuous function.

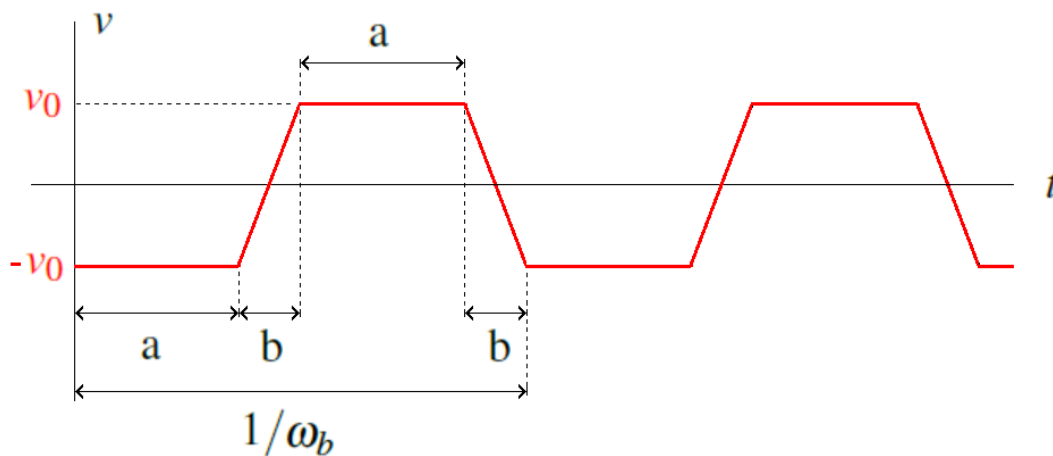


Figure 6: Periodic but no non-smooth belt speed.

### 3.2.1 Belt with continuous non-smooth speed

Considering the case when  $a \rightarrow 0$ , Eq. 13 can be rewritten as

$$v(t) = \begin{cases} -v_0 + 4v_0\omega_b t, & \text{if } t \in [0, 1/2\omega_b); \\ 3v_0 - 4v_0\omega_b t, & \text{if } t \in [1/2\omega_b, 1/\omega_b). \end{cases} \tag{14}$$

Fig. 7(a), 7(b), 8(a), 8(b), 9(a) and 9(b) show the phase diagram for the stick-slip oscillator in the steady state when  $v$  is given by Eq. 14 for different ratios,  $r = \omega_b/\omega_n$ . The positions corresponding to the stick mode are marked in red.

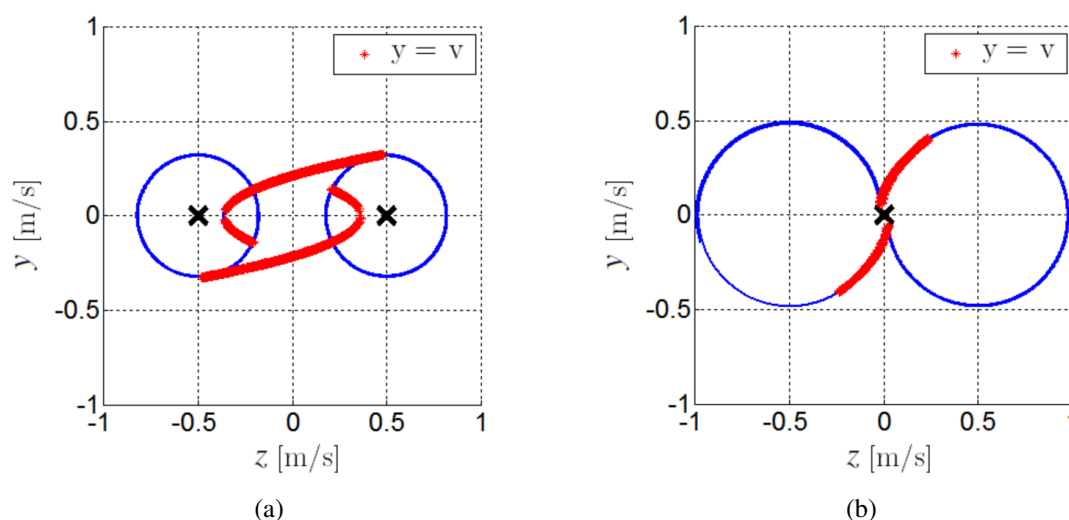


Figure 7: Belt with continuous and non-smooth speed: phase diagram for the stick-slip oscillator in the steady state with (a)  $\omega_b/\omega_n = 0.1$  and (b)  $\omega_b/\omega_n = 0.5$ .

### 3.2.2 Belt with periodic discontinuous speed

Considering the case when  $b \rightarrow 0$ , Eq. 13 can be rewritten as

$$v(t) = \begin{cases} -1, & \text{if } t \in [0, 1/2\omega_b); \\ 1, & \text{if } t \in [1/2\omega_b, 1/\omega_b). \end{cases} \quad (15)$$

The system behavior with this imposed discontinuous belt speed (a sort of bang-bang control) is affected by the ratio  $r = \omega_b/\omega_n$ .

To understand this influence, we start recalling the analytical form of the phase diagram when the belt has a constant speed,  $v$ . If the initial condition,  $|\dot{x}(0)| > |v|$ , the system will have a non steady state solution (in which occurs the stick mode) and after it, it will have a steady state solution (in which occurs the slip mode). If  $|\dot{x}(0)| \leq |v|$ , the system will have only a steady state solution. As it was explained in section 2, in the steady state solution, the block path is a circle with origin in the equilibrium point, Eq. 5, and with radius related with the block initial conditions.

Now, we return to the case of belt with discontinuous speed. Each change of the speed sign can be understood as a reboot of the system. Thus, the block position and velocity in the instant that there is change of the speed sign behave as initial conditions to the next time-interval (with size  $1/2\omega_b$ ) in which the belt speed is constant. The parameter  $2\omega_b$  determines the frequency in which the system is rebooted.

The case of small ratio  $r$ , that is,  $\omega_b$  is relatively small when compared with  $\omega_n$ , is illustrated in Fig. 10(a) and 10(b). In these figures, the block path when the belt speed is positive is drawn in green and when is negative is drawn in purple. It is possible to observe that, in both graphs, the block path is composed by circles with center at the equilibrium points  $(n\mu/m\omega_n, 0)$  and  $(-n\mu/m\omega_n, 0)$ . For  $r$  small, each time-interval (with size  $1/2\omega_b$ ) in which the belt speed is constant is long enough to allow the system response to reach the steady state (corresponding to the case in which the belt speed is always constant), that is, a complete circle in the phase diagram. For the ratio  $r = 0.1$  there is only one circle around each equilibrium point. For the ratio  $r = 0.4$  is different, there are two circles around each equilibrium point. Also, it is

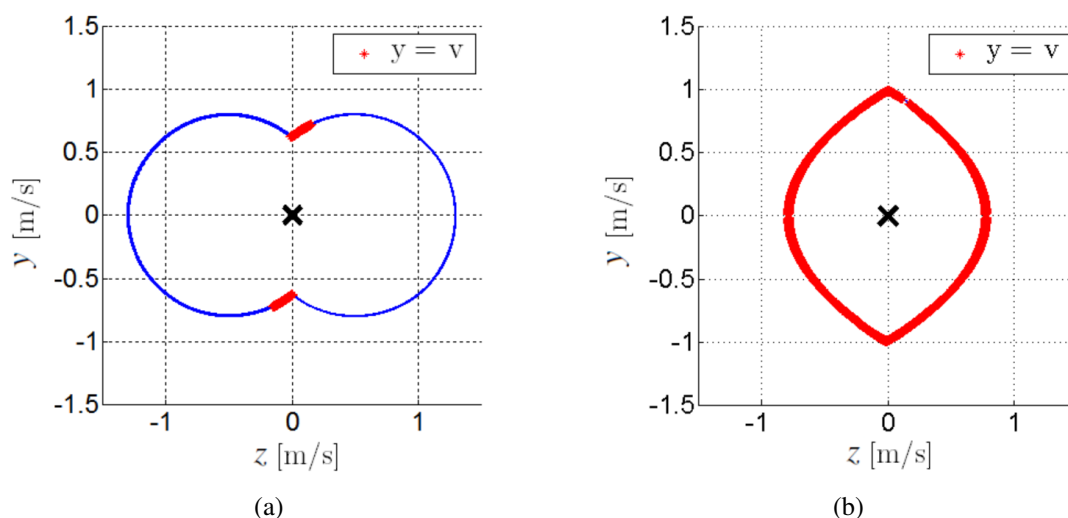


Figure 8: Belt with continuous and non-smooth speed: phase diagram for the stick-slip oscillator in the steady state with (a)  $\omega_b/\omega_n = 0.7$  and (b)  $\omega_b/\omega_n = 1.0$ .

possible to observe that there is no stick mode during the steady-state of the system.

When the ratio  $r$  is bigger, the phase diagram of the system is not anymore composed by complete circles with center at the equilibrium points  $(n\mu/m\omega_n, 0)$  and  $(-n\mu/m\omega_n, 0)$ , as shown in Fig. 11(a), 11(b), 12(a) and 12(b). This happens because each time-interval (with size  $1/2\omega_b$ ) in which the belt speed is constant is not long enough to allow the block to complete one turn around each equilibrium point.

In the case of ratio  $r = 1.0$  and  $r = 1.3$ , by the numerical results, it was verified that it can occurs the stick and slip modes in the steady state solution of the system. Thus, the phase diagram is composed by arcs of the circles with origin in  $(n\mu/m\omega_n, 0)$  and  $(-n\mu/m\omega_n, 0)$  (corresponding to the slip mode) and by horizontal straight segments (corresponding to the stick mode).

In the case of ratio  $r = 2.0$  and  $r = 2.5$ , it was verified that there is only slip mode in the steady state solution of the system. Thus, the phase diagram is composed only by arcs of the circles with origin in  $(n\mu/m\omega_n, 0)$  and  $(-n\mu/m\omega_n, 0)$ .

### 3.3 Belt with discontinuous friction coefficient

In this part of the paper, we would like to analyze the situations in which the belt has different surface conditions along its length, that is, the friction coefficient changes along the belt length. For example, parts of the belt are lubricated while others parts are not lubricated or, the belt is made of different materials intercalated. In all situations, depending on the part of the belt that is in contact with the block, we have a different friction coefficient.

We model the friction coefficient as a periodic (with frequency  $\omega_b$ ) and discontinuous function that can assume only two values  $\mu_1$  and  $\mu_2$  (representing, for example, the different conditions of the belt surface: lubricated and non lubricated). This function is written as

$$\mu(u) = \begin{cases} \mu_1, & \text{if } u \in [0, 1/2\omega_b); \\ \mu_2, & \text{if } u \in [1/2\omega_b, 1/\omega_b). \end{cases} \quad (16)$$

Similar to what happened in the case of belt with discontinuous speed, each change of the friction coefficient can be understood as a reboot of the system. Thus, the block position and

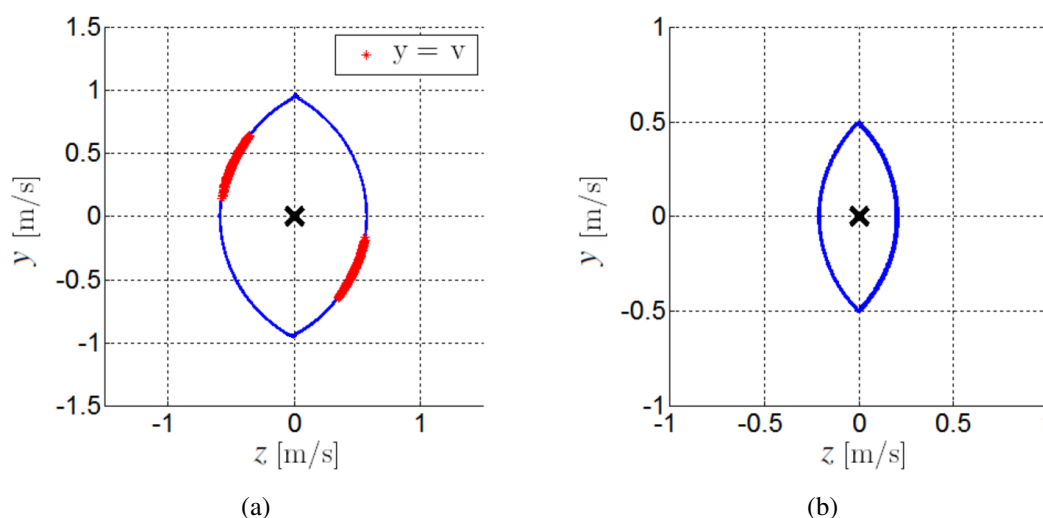


Figure 9: Belt with continuous and non-smooth speed: phase diagram for the stick-slip oscillator in the steady state with (a)  $\omega_b/\omega_n = 1.4$  and (b)  $\omega_b/\omega_n = 2.0$ .

velocity in the instant that there is a discontinuity in the friction coefficient behave as initial conditions to the next space-interval (with size  $1/2\omega_b$ ) in which the friction coefficient is constant. The parameter  $2\omega_b$  determines the frequency in which the system is rebooted.

By numerical simulations, it was verified that the system behavior with this discontinuous friction coefficient is affected by the ratio  $r = \omega_b/\omega_n$ . In the simulations, we analyze the situations in which the belt is made of two different materials intercalated (cast iron and steel), we also considered that the block is made of cast iron. Thus, the values used to  $\mu_1$  and  $\mu_2$  were respectively 1.1 (the friction coefficient between two cast iron surfaces) and 0.4 (the friction coefficient between a steel surface and a cast iron surface) (Blau, 2009).

The numerical simulations results show that when  $\omega_b$  is an integer multiple of  $\omega_n$ , that is, ratio  $r$  is an integer number, the stick-slip oscillator reaches a steady state solution. Otherwise, it do not reach a steady state solution in the range interval in which the Eq. (1) was integrated ( $[0, 400]$  seconds).

Figures 13(a), 13(b), 14(a) and 14(b) show the phase diagram for the stick-slip oscillator in the steady state solution with ratio  $r$  equal to 1.0, 2.0, 3.0 and 4.0 respectively. In these figures, the block path when the friction coefficient is  $\mu_1$  is drawn in green and when is  $\mu_2$  is drawn in purple. In all graphs, it is possible to observe that the block path is composed by circles with origin at the equilibrium points  $(n\mu_1/m\omega_n, 0)$  and  $(-n\mu_2/m\omega_n, 0)$ .

Figures 15(a), 15(b), 16(a) and 16(b) show the phase diagram during the last half part of the simulation for four different not integer values of  $r$ .

#### 4 STOCHASTIC MODEL OF THE COULOMB FRICTION

As it was explained in the introduction, to construct a model of the frictional force is not a simple task. To deal with the friction coefficient variability and the friction dependency on the relative velocity of the bodies in contact, we propose to analyze the stick-slip oscillator with a stochastic approach.

Two different sources of uncertainties are investigated separately. In the first one, it is assumed that the randomness is only in the belt speed. In the second one, that it is only in the friction coefficient. As this paper is a first work of the stick-slip oscillator with a random fric-

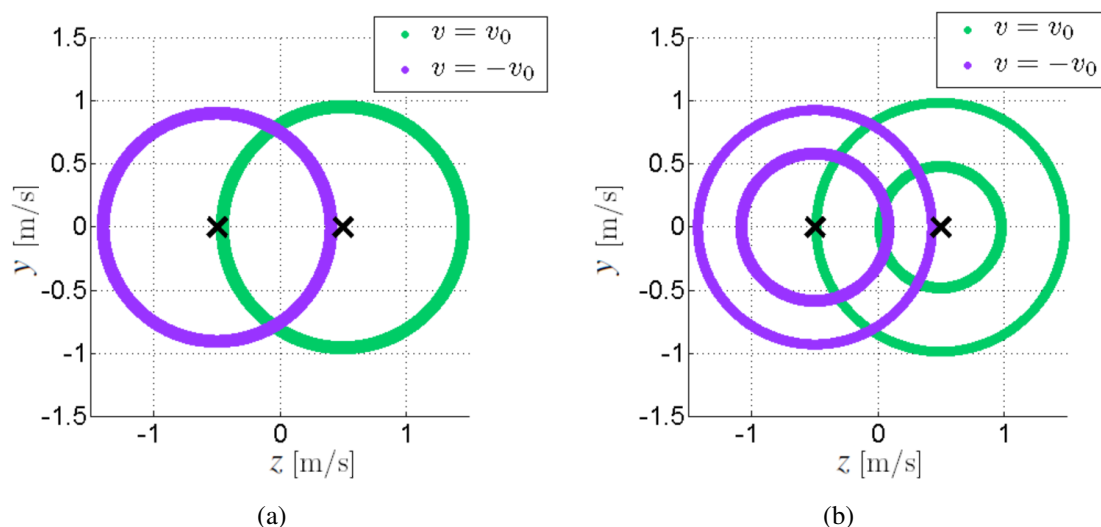


Figure 10: Belt with discontinuous speed: phase diagram for the stick-slip oscillator in the steady state solution with (a)  $\omega_b/\omega_n = 0.1$  and (b)  $\omega_b/\omega_n = 0.4$ .

tion, this simplified strategy to separate the uncertainty sources is adopted. In future works, both sources should be investigated together.

#### 4.1 Random belt speed

Considering that the belt speed is the only source of uncertainty in the stick-slip oscillator problem, we propose to treat it as a random process with parameter  $t$  constant by parts, represented by  $\mathcal{V}$ . Thus, we define  $\mathcal{V}$  as a finite collection of real-valued random variables  $\{V_1, V_2, \dots, V_n, \dots\}$ ,  $\forall n \in \mathbb{N}$ , from a probability space  $(\Omega, \mathcal{F}, P)$ , where  $\Omega$  is the sample space,  $\mathcal{F}$  is the  $\sigma$ -algebra and  $P$  is the probability measure.

As it is assumed that  $\mathcal{V}$  is random process constant by parts, given a time-interval with size  $1/\omega_b$ ,

$$\mathcal{V}(t) = V_n \quad \text{if } t \in \left[ \frac{n-1}{\omega_b}, \frac{n}{\omega_b} \right], \quad \forall n \in \mathbb{N}. \quad (17)$$

Beside this, it is assumed that  $\{V_1, V_2, \dots, V_n, \dots\}$  is a collection of equal and discrete random variables, in which each  $V_n$  can have only the values  $-v_0$  and  $v_0$  with equal probability.

#### 4.2 Random frictional coefficient

Considering that the frictional coefficient is a source of uncertainty in the stick-slip oscillator problem, we would like to represent the situations in which the belt has random surface conditions along its length.

In section 3.3, cases in which the belt has different friction coefficients along its length were analyzed. Here, it is different, we analyze situations in which friction coefficient changes randomly along the belt length.

To construct a stochastic model of the friction coefficient that represent these kind of situations, we propose to model it as a random field, represented by  $\mathcal{M}$ , with parameter  $x$  on  $[0, l]$ , where  $l$  is the belt length. Two different probability models were developed to this random field.

In the first one, it is assumed that  $\mathcal{M}$  is a random field constant by parts. As done in the previous case,  $\mathcal{M}$  is defined as a finite collection of equal and discrete real-valued random

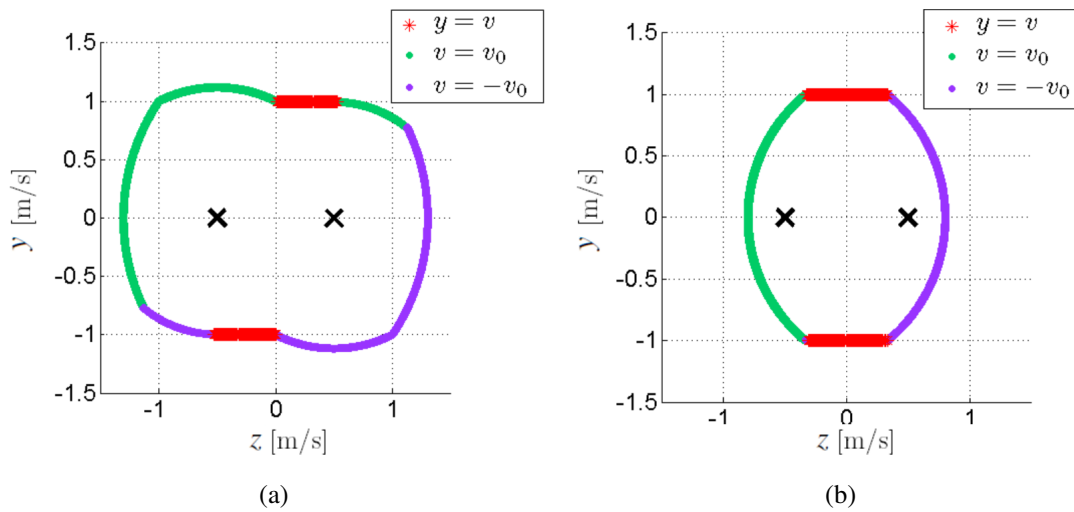


Figure 11: Belt with discontinuous speed: phase diagram for the stick-slip oscillator in the steady state solution with (a)  $\omega_b/\omega_n = 1.0$  and (b)  $\omega_b/\omega_n = 1.3$ .

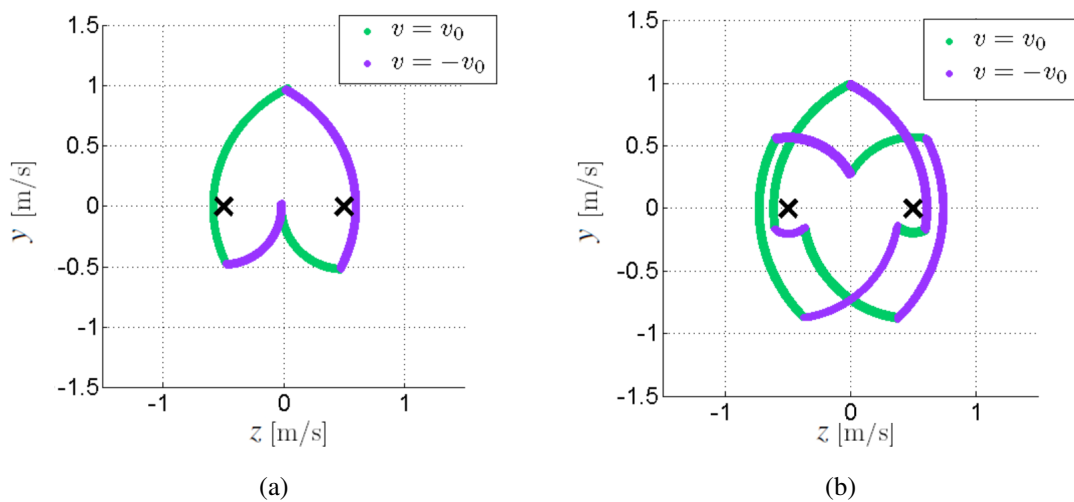


Figure 12: Belt with discontinuous speed: phase diagram for the stick-slip oscillator in the steady state solution with (a)  $\omega_b/\omega_n = 2.0$  and (b)  $\omega_b/\omega_n = 2.5$ .

variables  $\{M_1, M_2, \dots, M_n, \dots\}, \forall n \in \mathbb{N}$ .

Given a space-interval with size  $1/\omega_b$ ,

$$\mathcal{M}(u) = M_n \quad \text{if } u \in \left[ \frac{n-1}{\omega_b}, \frac{n}{\omega_b} \right], \quad \forall n \in \mathbb{N}. \quad (18)$$

It is assumed also that each discrete random variable in the collection  $\{M_1, M_2, \dots, M_n, \dots\}$  can have only the values  $\mu_1$  and  $\mu_2$  with equal probability. This two values represent the different conditions of the belt surface, for example, lubricated and non lubricated.

In the second model constructed to the random frictional coefficient field, it is assumed that  $\mathcal{M}$  is a stationary truncated Gaussian random field with exponential autocorrelation function

$$R(u_1, u_2) = \sigma^2 \exp\left(-\frac{|u_2 - u_1|}{b}\right). \quad (19)$$

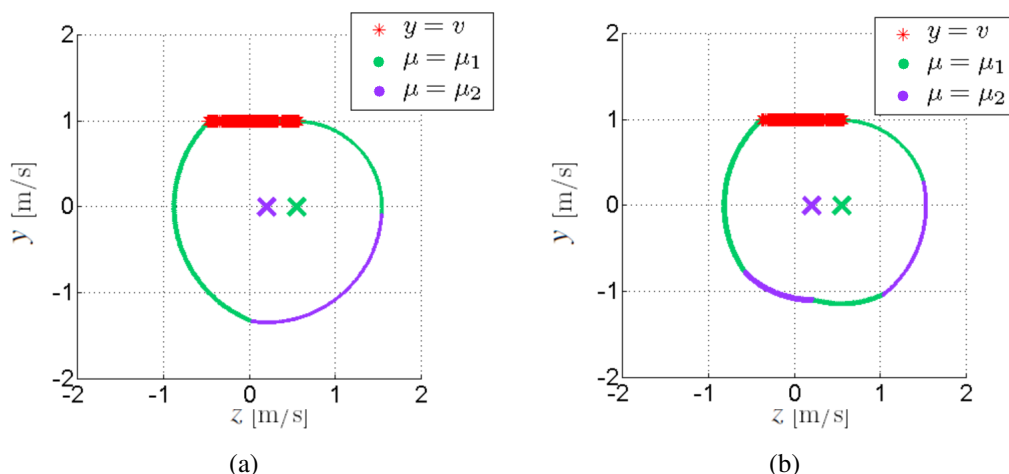


Figure 13: Belt with discontinuous friction coefficient: phase diagram for the stick-slip oscillator in the steady state solution with (a)  $\omega_b/\omega_n = 1.0$  and (b)  $\omega_b/\omega_n = 2.0$ .

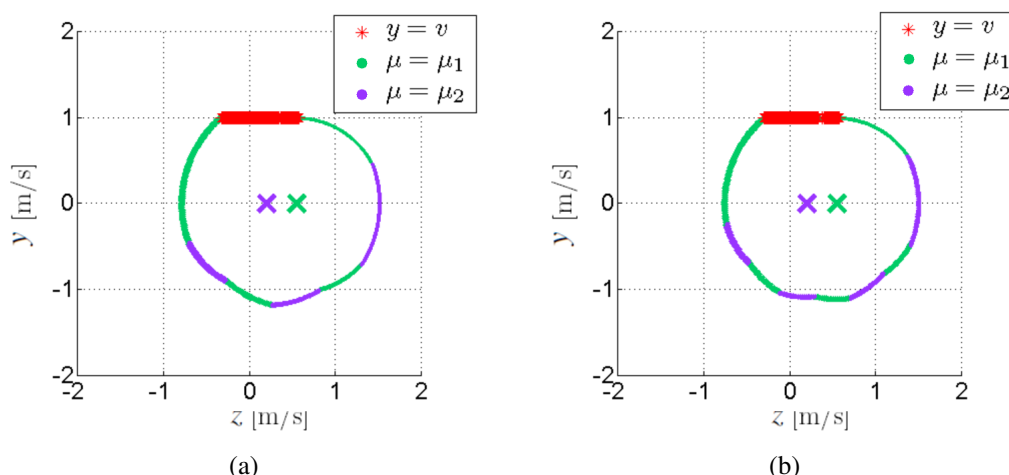


Figure 14: Belt with discontinuous friction coefficient: phase diagram for the stick-slip oscillator in the steady state solution with (a)  $\omega_b/\omega_n = 3.0$  and (b)  $\omega_b/\omega_n = 4.0$ .

where  $b$  is the correlation length, which measures the decay of the autocorrelation function. This stochastic model to the random frictional coefficient field was proposed by (Ritto et al., 2013; Choi et al., 2011).

The stochastic field  $\mathcal{M}$  is then expanded using the Karhunen-Loève expansion (Karhunen, 1947; Loève, 1977; Sampaio and Lima, 2012)

$$\mathcal{M}(u, \xi) = \mu(u) + \sum_{k=1}^n \sqrt{\lambda_k} \phi_k(x) Z_k(\xi), \tag{20}$$

where  $\mu$  is the mean value of the frictional coefficient,  $\lambda_k$  and  $\phi_k$  are the  $k$ -th eigenvalue and  $k$ -th eigenvector of the autocorrelation function  $R$  and  $Z_k$  are independent standard Gaussian random variables. The number of terms considered in the expansion,  $n$ , defines the precision of this representation.

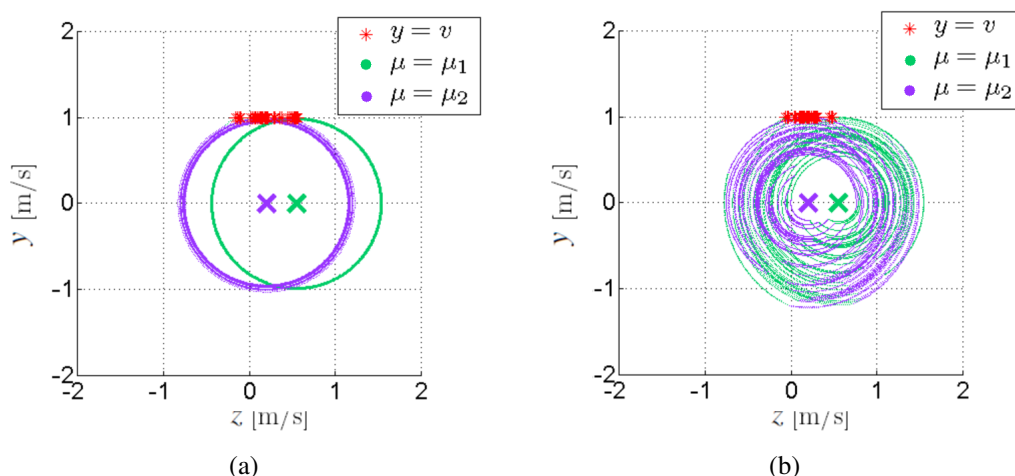


Figure 15: Belt with discontinuous friction coefficient: phase diagram for the stick-slip oscillator (during the last half part of the simulation) with (a)  $\omega_b/\omega_n = 0.5$  and (b)  $\omega_b/\omega_n = 1.5$ .

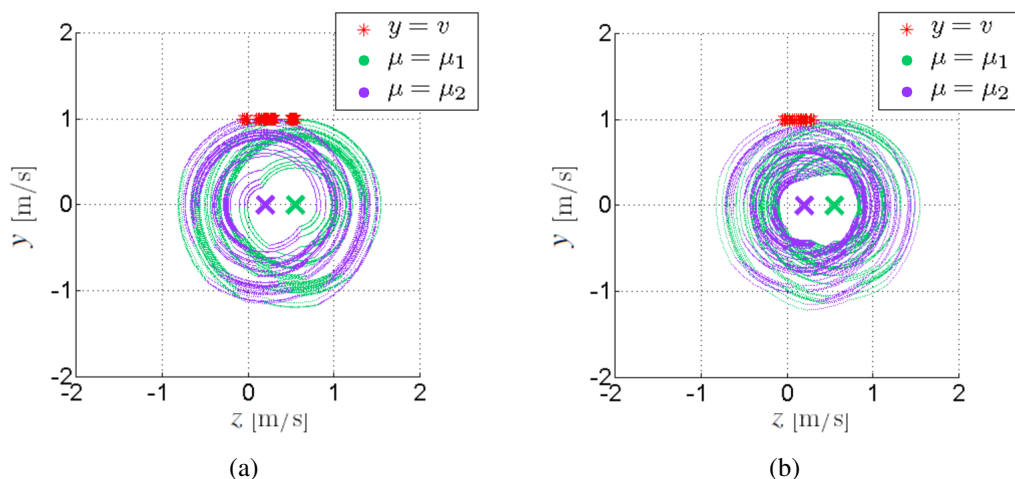


Figure 16: Belt with discontinuous friction coefficient: phase diagram for the stick-slip oscillator (during the last half part of the simulation) with (a)  $\omega_b/\omega_n = 2.5$  and (b)  $\omega_b/\omega_n = 3.5$ .

## 5 NUMERICAL SIMULATIONS OF THE STICK-SLIP OSCILLATOR WITH RANDOM COULOMB FRICTION

As it was assumed that the belt speed or the friction coefficient are uncertain, the response of the stochastic stick-slip oscillator is a random process with parameter  $t$  and thus, the equation of motion of the system, Eq. 1, became a stochastic differential equation. The block displacement is represented by the random process  $\mathcal{X}$  and its velocity by  $\dot{\mathcal{X}}$ .

To make the stochastic analysis of the system, Monte Carlo simulations were employed to compute statistics of the response of  $\mathcal{X}$  and  $\dot{\mathcal{X}}$ .

### 5.1 Random belt speed

In this section, we consider that the belt speed is the only source of uncertainty in the stick-slip oscillator problem and it is modeled as a random process constant by parts,  $\mathcal{V}$ , as described in Eq. 17, and consider that its values  $-v_0$  and  $v_0$  are respectively  $-1.0$  and  $1.0$ .

Figures 17(a), 17(b), 18(a) and 18(b) show the envelope graphs of  $\dot{\mathcal{X}}$  constructed with 100

realizations of it with different ratios  $r = \omega_b/\omega_n$ . In each simulation, it were considered as initials conditions to the block  $x(0) = 0$  [m] and  $\dot{x}(0) = 1.0$  [m/s].

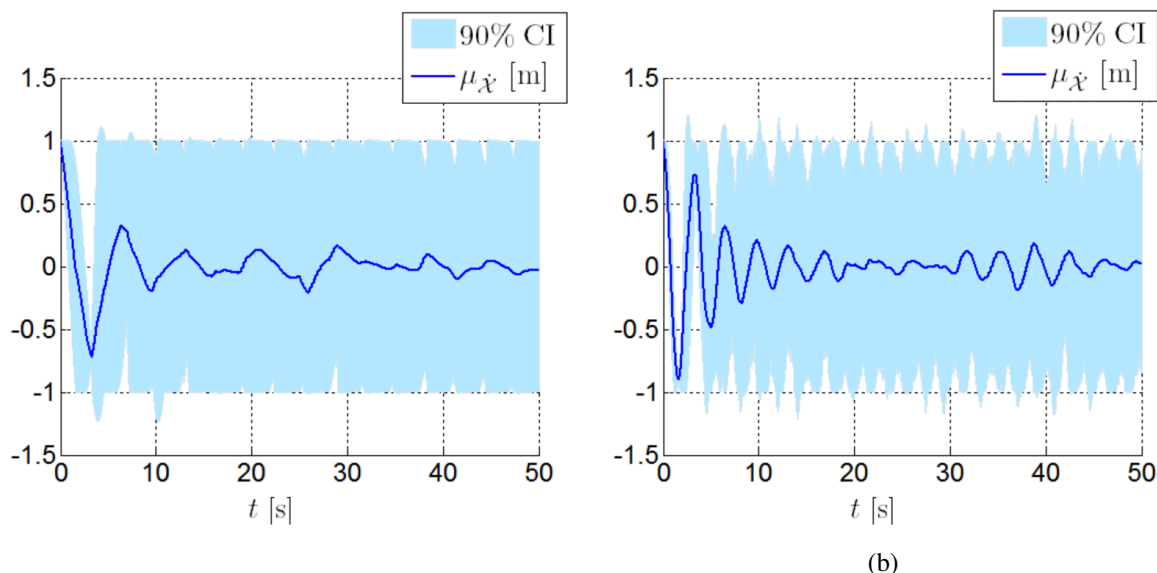


Figure 17: Random belt speed: envelope graphs of  $\dot{X}$  with initials conditions  $x(0) = 0$  [m] and  $\dot{x}(0) = 1.0$  [m/s] for (a)  $r = 0.5$  and (b)  $r = 0.8$ .

Changing the block initial conditions to  $x(0) = 0$  [m] and  $\dot{x}(0) = 0$  [m/s], two interesting phenomena can be verified by the envelope graphs of  $X$  and  $\dot{X}$ . Depending on the ratio  $r$ , it is possible that in some instants,  $t^*$ , there is no dispersion on the block position and in some other instants,  $t^{**}$ , there is no dispersion on the block velocity.

When, for example,  $r = 0.6$ , this phenomena of no dispersion on the block position occur in one instant,  $t^* = 1/\omega_b$  [s]. The phenomena of no dispersion on the block velocity occur in three instants:  $t_1^{**} = 1/(2\omega_b)$  [s],  $t_2^{**} = 1/\omega_b$  [s] and  $t_3^{**} = 3/(2\omega_b)$  [s]. Figures 19(a) and 19(b) illustrate the envelope graphs of  $X$  and  $\dot{X}$ , constructed with 200 realizations of each one of these random process.

When  $r = 1.0$ , in every instant  $t^*$  multiple of  $1/\omega_b$ , happens the phenomena of no dispersion on the block position. In every instant  $t^{**}$  multiple of  $1/(2\omega_b)$ ,  $1/\omega_b$ ,  $3/(2\omega_b)$  and  $2/\omega_b$  happens the phenomena of no dispersion on the block velocity. Also, the envelope graphs of  $X$  and  $\dot{X}$  became symmetric with respect to the time axis, as shown in Fig. 20(a) and 20(b).

When  $r < 1.0$ , these phenomena of no dispersion on the block position and velocity do not occurs, as it is illustrated in the envelope graphs of Fig. 21(a) and 21(b), constructed with 200 realizations of  $X$  for two different values of  $r$ .

## 5.2 Random frictional coefficient

In the first part this section, we consider that the frictional coefficient is the only source of uncertainty in the stick-slip oscillator problem and it is modeled as a random field constant by parts,  $\mathcal{M}$ , as described in Eq. 18. With this model, we represent a belt that is made of different materials intercalated.

We consider that the block is made of cast iron and the belt is made of sections of cast iron and sections of steel intercalated. The values used to  $\mu_1$  and  $\mu_2$  were are respectively 1.1 (the

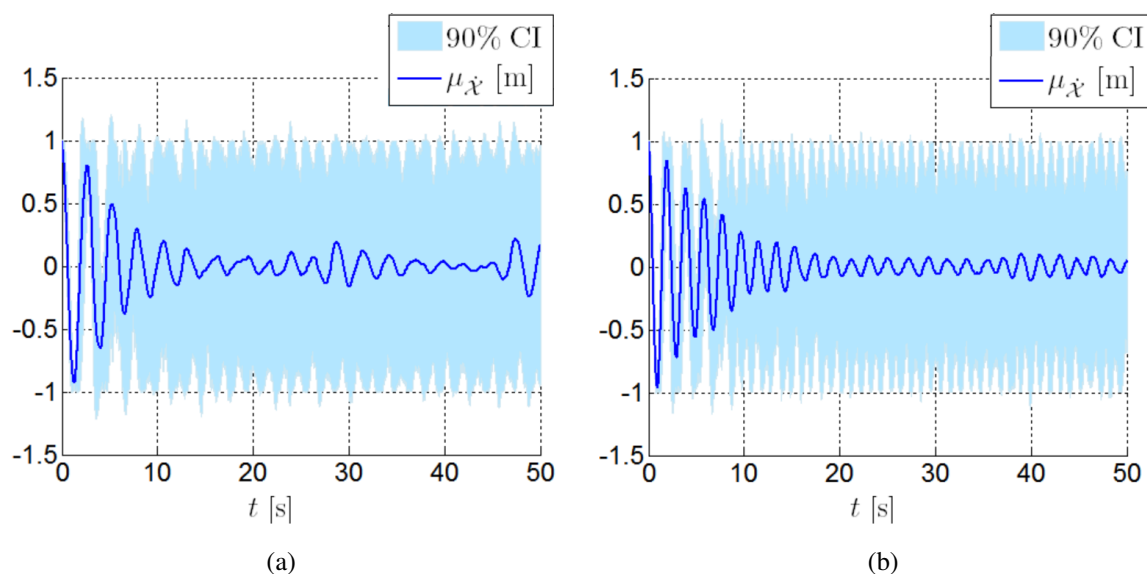


Figure 18: Random belt speed: envelope graphs of  $\dot{X}$  with initial conditions  $x(0) = 0$  [m] and  $\dot{x}(0) = 1.0$  [m/s] for (a)  $r = 1.0$  and (b)  $r = 1.5$ .

friction coefficient between two cast iron surfaces) and 0.4 (the friction coefficient between cast iron surface and a steel surface) (Blau, 2009).

Figures 22(a), 22(b), 23(a) and 23(b) show the envelope graphs of  $\dot{X}$  constructed with 100 realizations of it with different ratios  $r = \omega_b / \omega_n$ .

In the second part this section, we consider that the frictional coefficient is a stationary truncated Gaussian random field,  $\mathcal{M}$ , with exponential autocorrelation function given by Eq. 19.

As this random field was expanded by the Karhunen-Loève expansion, the generation of its samples used in the Monte Carlo simulations was made by sampling the random variables  $Z_k$  of the expansion. The mean value of the frictional coefficient,  $\mu$ , was assumed to be a constant function with value 1.1. The value used to the correlation length,  $b$ , was 0.01 and to  $\sigma$  the value was 3. The belt length was 1.0 [m].

To compute the eigenvalues and eigenvectors of the autocorrelation function  $R$ , Eq. 19, first, we construct a spacial grid on belt length with spacial-step equal to  $\delta u = 10^{-3}$  [m], that is, we construct the vector  $\{u\}$  ( $d \times 1$ ), with  $d = 1.001$ . After it, we construct a matrix  $[R]$  ( $d \times d$ ), in which each element  $R_{ij}$  is equal to  $\sigma^2 \exp(-|u_j - u_i|/b)$ . Approximations to the eigenvalues,  $\hat{\lambda}$ , and eigenvectors,  $\{\hat{\phi}\}$ , of  $[R]$  were computed solving the following eigenvalue problem (Sampaio and Lima, 2012)

$$[R] \{\hat{\phi}\} \delta u = \hat{\lambda} \{\hat{\phi}\} . \quad (21)$$

Figures 24(a) and 24(b) show the envelope graphs of  $X$  and  $\dot{X}$  constructed with 200 realizations of these random process. In each realization, the block initial conditions were  $x(0) = 0.0$  [m] and  $\dot{x}(0) = 0.0$  [m/s].

## 6 CONCLUSIONS

The purpose of this paper was to better understand stick-slip oscillators hoping that the better knowledge would help to optimize the drilling process. The focus was in the steady-state, when one was found because it could be reproduced, and this way one could be assured of the

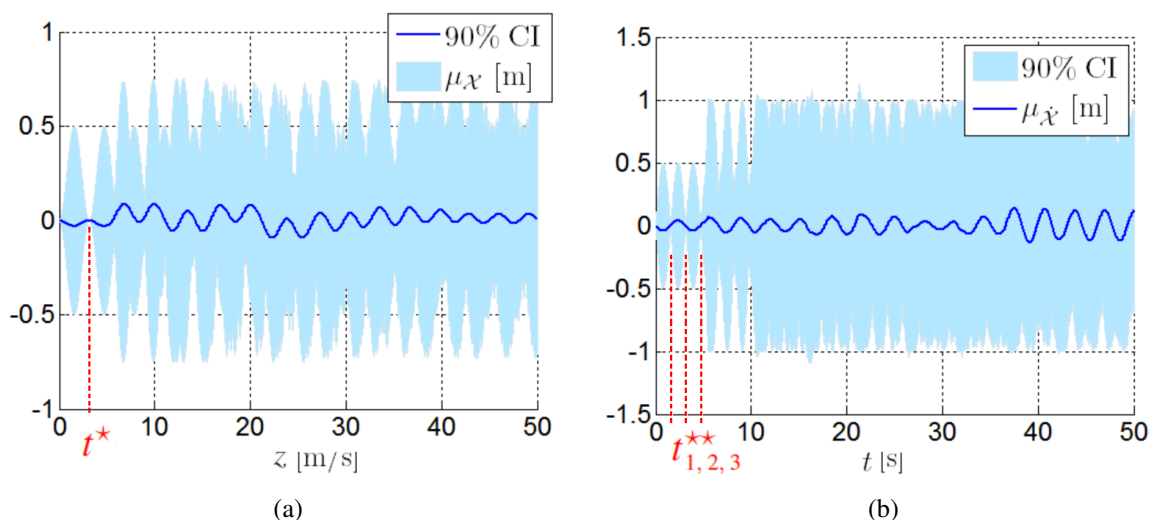


Figure 19: Random belt speed: with initials conditions  $x(0) = 0$  [m] and  $\dot{x}(0) = 0.0$  [m/s] and  $r = 0.6$ . Envelope graphs of (a)  $X$  and (b)  $\dot{X}$ .

results. Except in some cases the Coulomb's model for friction was used in the simulations. Deterministic and stochastic situations were analyzed and the focus was in finding the stick-and-slip-mode parts of a trajectory. The driving force, the belt motion, was imposed in different ways, in time and space. That is, the velocity of the belt was varied in time and its configuration was uniform and also piecewise uniform. The friction between block-belt is very complex and can only be coarsely described. However, the Coulomb's friction model is surprisingly good in describing the non-smooth dynamics of a stick-slip oscillator. Maybe the mechanism is not the same, but the dynamics of a simple stick-slip oscillator mimics that found in the drilling process.

In the deterministic analysis of the stick-slip oscillator with a constant belt speed and the same surface conditions along its length, it is verified that considering only the steady state solution, there is no stick mode in, when the Coulomb's model is used. The block oscillates around an equilibrium point related with the normal force exerted on the block, the friction coefficient and the natural frequency of system.

When the belt has a different imposed periodic speed, as harmonic speed, continuous and non-smooth speed or discontinuous speed, it is verified, by numerical simulations, that the stick mode can occur in the steady state of the system, depending on the ratio  $r$  between the frequency of the belt speed and the natural frequency of the system. In the cases of the harmonic speed and of continuous and non-smooth speed, with  $r = 1.0$ , the stick mode occurs during the entire steady state solution of the system, i.e., there is no slip.

When the belt has different surface conditions along its length, featuring the friction coefficient between the belt and the block as a discontinuous function along the belt length, it is verified, also by numerical simulations, that the presence of stick and slip mode in the steady state of the system depends on the ratio  $r$  between the spatial frequency of the friction coefficient function and the natural frequency of the system. For integer values of the ratio  $r$ , the system reaches a steady state solution and presents the stick mode during part of its path. For not integer values of  $r$ , the system do not reach a steady state solution.

In the stochastic analysis, assuming that the randomness is in the belt velocity, modeling it as a random process piecewise uniform (characterized by the time-interval  $1/\omega_b$ ) and considering

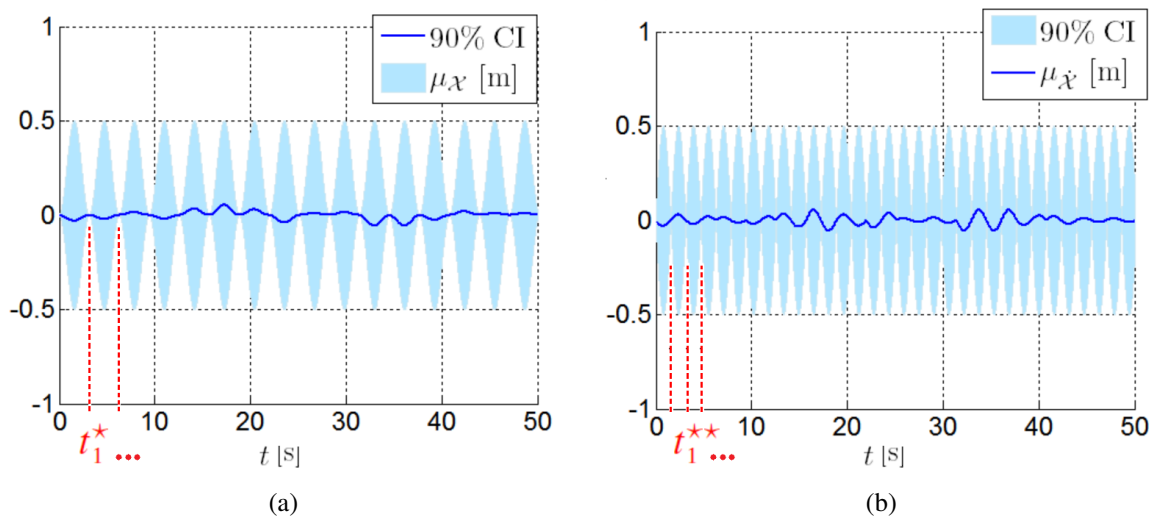


Figure 20: Random belt speed: with initials conditions  $x(0) = 0$  [m] and  $\dot{x}(0) = 0.0$  [m/s] and  $r = 1.0$ . Envelope graphs of (a)  $X$  and (b)  $\dot{X}$ .

zero initial conditions to the block, two interesting phenomena were verified in the envelope graphs of the block displacement and velocity. Depending on the ratio  $r$ , between  $\omega_b$  and the natural frequency of the system, it is possible that in some instants there is no dispersion on the block position and velocity. When  $r = 1.0$ , in every instant multiple of  $1/\omega_b$  there is no dispersion on the block position, and in every instant multiple of  $1/(2\omega_b)$ ,  $1/\omega_b$ ,  $3/(2\omega_b)$  and  $2/\omega_b$  there is no dispersion on the block velocity.

This is an ongoing work, and there are still many investigation to perform with this stick-slip oscillator to help to optimize drilling process. For instance, a refinement of the system model (making it closer to a real drillstring), a refinement of the stochastic modeling and a robust optimization to maximize the performance of the drilling process considering the uncertainties in the friction model.

## 7 ACKNOWLEDGMENTS

This work was supported by the Brazilian Agencies CNPQ, CAPES and FAPERJ.

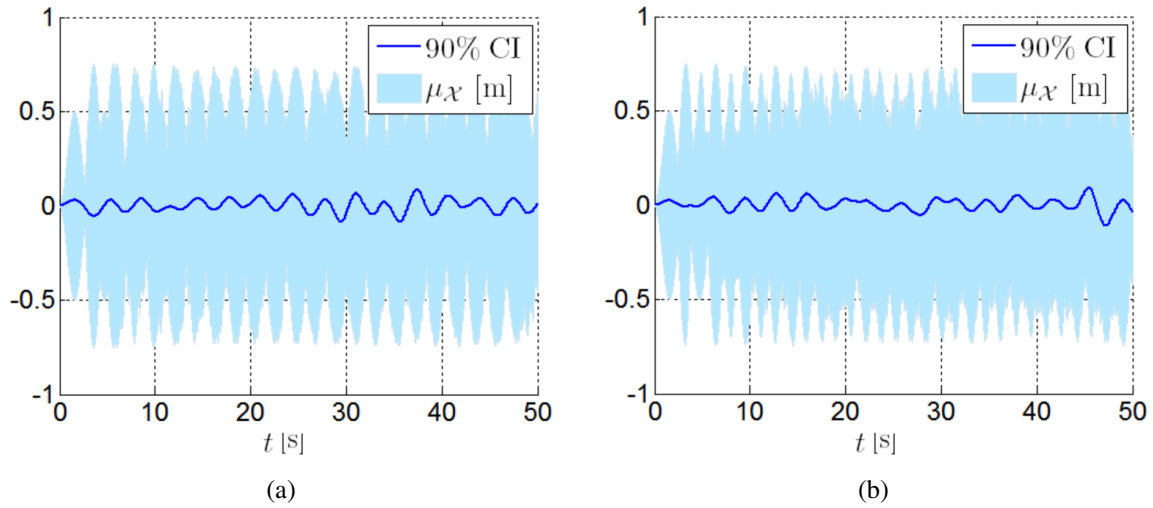


Figure 21: Random belt speed: envelope graphs of  $\dot{x}$  with initials conditions  $x(0) = 0$  [m] and  $\dot{x}(0) = 0.0$  [m/s] for (a)  $r = 1.5$  and (b)  $r = 2.0$ .

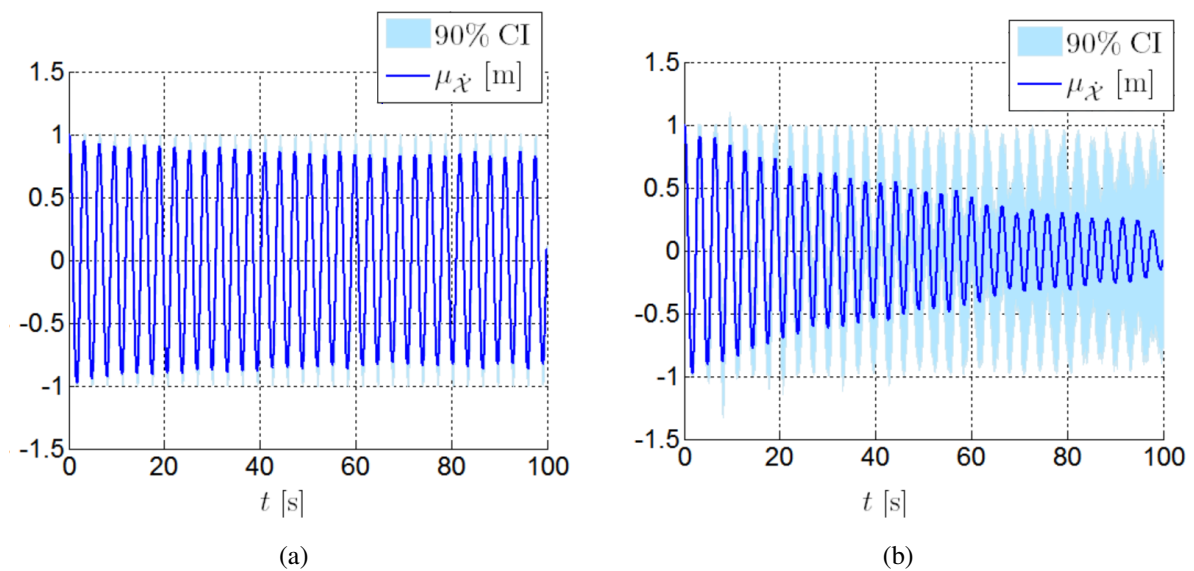


Figure 22: Random frictional coefficient (random field constant by parts): envelope graphs of  $\dot{x}$  with (a)  $r = 0.5$  and (b)  $r = 0.6$ .

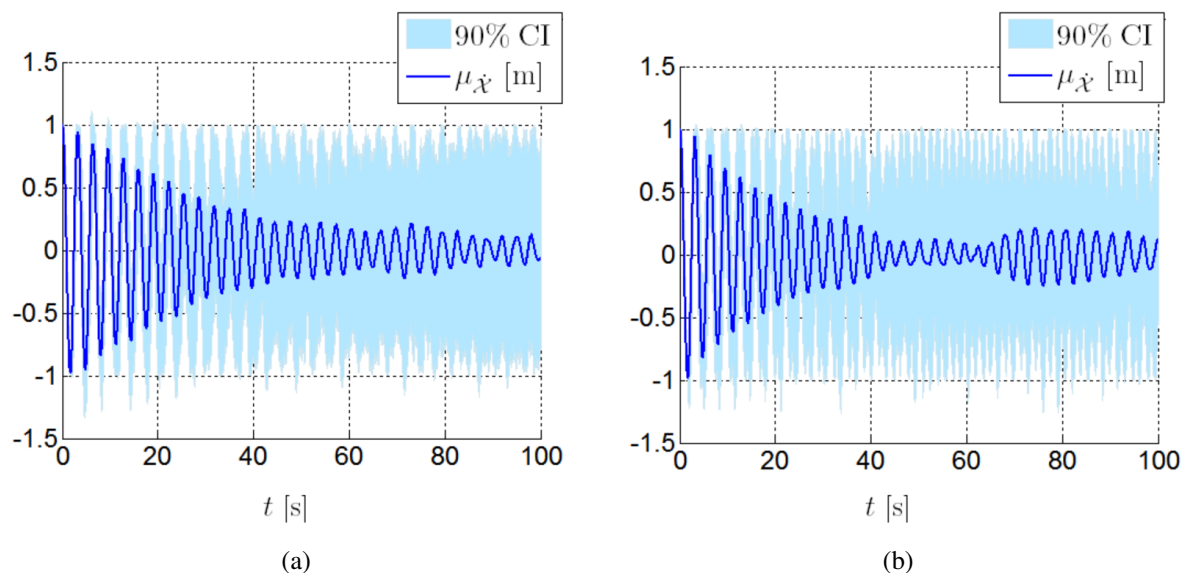


Figure 23: Random frictional coefficient (random field constant by parts): envelope graphs of  $\ddot{X}$  with (a)  $r = 0.8$  and (b)  $r = 1.0$  .

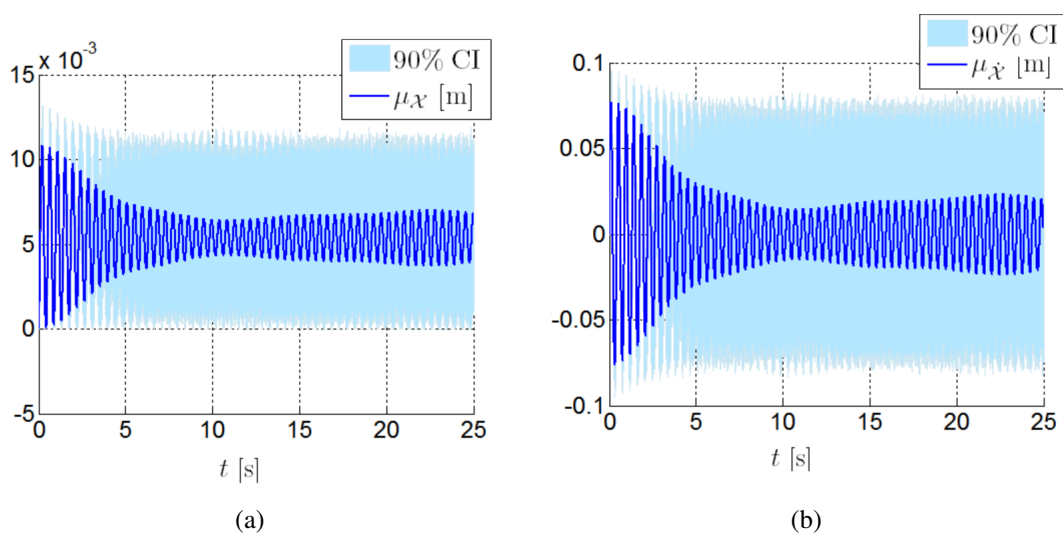


Figure 24: Random frictional coefficient (stationary truncated Gaussian random field): envelope graphs of (a)  $\ddot{X}$  and (b)  $\ddot{X}$  with a belt speed constant in time .

**REFERENCES**

- Berger E. Friction modeling for dynamic system simulation. *Appl Mech Rev*, 52(6), 2002.
- Blau P. *Friction science and technology: from concepts to applications*. CRC Press, Society of Tribologists and Lubrication Engineers, second edition, 2009.
- Choi B.K., Sipperley M., Mignolet M., and Soize C. Discrete maximum entropy process modeling of uncertain properties: application to friction for stick-slip and microslip response. *EURODYN2011, 8th International Conference on Structural Dynamics*, 2011.
- Cortet P., Dalbe M., Guerra C., Cohen C., Ciccotti M., Santucci S., and Vanel L. Intermittent stick-slip dynamics during the peeling of an adhesive tape from a roller. *Physical Review*, 87:022601–1–8, 2013.
- Csernák G. and Stépán G. On the periodic response of a harmonically excited dry friction oscillator. *Journal of Sound and Vibration*, 295:649 – 658, 2006.
- Feeny B., Guran A., Hinrichs N., and Popp K. A historical review on dry friction and stick-slip phenomena. *Appl Mech Rev*, 51(5), 1998.
- Feng Q. A discrete model of a stochastic friction system. *Comput. Methods Appl. Mech. Engrg.*, 192:2339 – 2354, 2003.
- Galvanetto U. and Bishop S. Dynamics of a simple damped oscillator undergoing stick-slip vibrations. *Meccanica*, 34:337–347, 1999.
- Jordan D.W. and Smith P. *Nonlinear ordinary differential equations: an introduction for scientists and engineers*. Oxford University Press, fourth edition, 2007.
- Karhunen K. On linear methods in probability and statistics. *Annales Academiae Scientiarum Fennicae Seried A.I. Mathematica-Physica*, 37:1–79, 1947.
- Loève M. *Probability Theory*. Graduate texts in mathematics. Springer, fourth edition, 1977.
- Navarro-López E.M. and Suárez R. Practical approach to modelling and controlling stick-slip oscillations in oilwell drillstrings. In IEEE, editor, *Proceedings of the 2004 IEEE, International Conference on Control Applications*, pages 1454–1460. IEEE, 2004.
- Poudou O. *Modeling and analysis of the dynamics of dry-friction-damped structural systems*. Ph.D. thesis, University of Michigan, 2007.
- Ritto T., Escalante M., Sampaio R., and Rosales M. Drill-string horizontal dynamics with uncertainty on the frictional force. *Journal of Sound and Vibration*, 332:145–153, 2013.
- Sampaio R. and Lima R. *Modelagem Estocástica e Geração de Amostras de Variáveis e Vetores Aleatórios*. Notas de Matemática Aplicada. SBMAC, <http://dx.doi.org/10.5540/001.2012.0070.01>, 2012.
- Tariku F. *Simulation of dynamic mechanical systems with stick-slip friction*. Ph.D. thesis, University of New Brunswick, 1998.
- Vahid-Araghi O. and Golnaraghi F. *Friction-induced vibration in lead screw drives*. Springer, 2010.
- Zaspa Y. Force characteristics of dry friction when contact oscillates. *Journal of Friction and Wear*, 30(1):17 – 24, 2009.